

Understanding and Guiding Weakly Supervised Entity Alignment with Potential Isomorphism Propagation

Yuanyi Wang
Beijing University of Posts and
Telecommunications
Beijing, China
wangyuanyi@bupt.edu.cn

Wei Tang
2012 Lab, Huawei Co. LTD
Beijing, China
tangocean@bupt.edu.cn

Haifeng Sun
Beijing University of Posts and
Telecommunications
Beijing, China
hfsun@bupt.edu.cn

Zirui Zhuang
Beijing University of Posts and
Telecommunications
Beijing, China
zhaungzirui@bupt.edu.cn

Xiaoyuan Fu
Beijing University of Posts and
Telecommunications
Beijing, China
fuxiaoyuan@bupt.edu.cn

Jingyu Wang
Beijing University of Posts and
Telecommunications
Beijing, China
wangjingyu@bupt.edu.cn

Qi Qi
Beijing University of Posts and
Telecommunications
Beijing, China
qiqi8266@bupt.edu.cn

Jianxin Liao
Beijing University of Posts and
Telecommunications
Beijing, China
jxlbupt@gmail.com

ABSTRACT

Weakly Supervised Entity Alignment (EA) is the task of identifying equivalent entities across diverse knowledge graphs (KGs) using only a limited number of seed alignments. Despite substantial advances in aggregation-based weakly supervised EA, the underlying mechanisms in this setting remain unexplored. In this paper, we present a propagation perspective to analyze weakly supervised EA and explain the existing aggregation-based EA models. Our theoretical analysis reveals that these models essentially seek propagation operators for pairwise entity similarities. We further prove that, despite the structural heterogeneity of different KGs, the potentially aligned entities within aggregation-based EA models have isomorphic subgraphs, which is the core premise of EA but has not been investigated. Leveraging this insight, we introduce a potential isomorphism propagation operator to enhance the propagation of neighborhood information across KGs. We develop a general EA framework, PipEA, incorporating this operator to improve the accuracy of every type of aggregation-based model without altering the learning process. Extensive experiments substantiate our theoretical findings and demonstrate PipEA’s significant performance gains over state-of-the-art weakly supervised EA methods. Our work not only advances the field but also enhances our comprehension of aggregation-based weakly supervised EA. The code and data are available at <https://github.com/wyy-code/PipEA>.

CCS CONCEPTS

• **Computing methodologies** → **Neural networks**; • **Information systems** → **Information integration**.

KEYWORDS

Entity Alignment, Knowledge Graphs, Weakly Supervised Learning, Propagation Operator, Potential Isomorphism Propagation

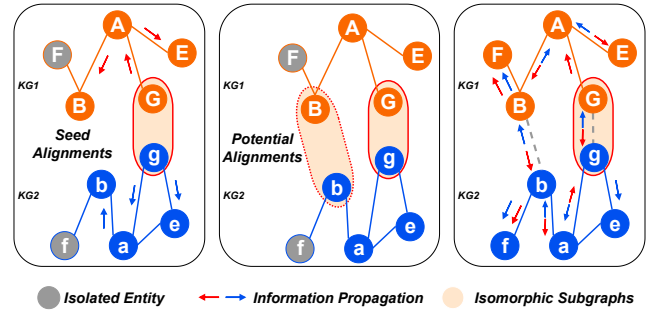


Figure 1: Fundamental limitation of aggregation-based models (Left) and our potential isomorphism propagation (Right).

1 INTRODUCTION

Knowledge Graphs (KGs) have emerged as pivotal resources across diverse domains, such as information retrieval [45], question answering [2], and recommendation systems [35]. Despite their growing importance, KGs suffer from limitations in coverage, constraining their utility in downstream applications. The integration of heterogeneous KGs presents a significant challenge, at the core of which lies Entity Alignment (EA). EA aims to identify corresponding entities across different KGs. Contemporary EA solutions, particularly aggregation-based models, adhere to established pipelines. They rely on abundant seed alignments as supervised signals to learn entity representations, projecting diverse KGs into a unified embedding space, and subsequently predicting alignment results using these unified embeddings.

However, these methods heavily hinge on the availability of substantial seed alignments, which can be unrealistic or expensive to obtain. This has led to increased interest in weakly supervised EA, a scenario where only a limited number of seed alignments are

accessible. Recent studies [1, 13, 24] have explored strategies like active learning and additional information incorporation to enhance the performance of aggregation-based EA models, which are state-of-the-art weakly supervised EA methods. While these efforts have shown some promise, it remains unclear why the adaptation of aggregation-based EA models for effective information propagation in weakly supervised settings is challenging.

This paper delves into weakly supervised EA, focusing on how to enhance aggregation-based EA models in weakly supervised settings through the perspective of information propagation. We unveil that potentially aligned entities exhibit isomorphic subgraphs. We analyze the limitations of existing models in weakly supervised contexts, noting their reliance on local structural information and iterative neighbor aggregation. These models aim to minimize the distances between output embeddings of seed alignments, as further elaborated in Section 3. Figure 1 (left) depicts the key challenge: reliance on a sufficient quantity of seed alignments like (G,g). Limited seed alignments result in many unlabeled entities can not utilize the prior knowledge from labeled ones, hampering the propagation of alignment information due to restricted aggregation steps. For instance, in a two-layer GNN, only entities within a two-hop radius (like A, B) of seed entities participate in aggregation-based propagation, leaving distant entities isolated.

While the concept of employing higher-order aggregation-based models to expand neighborhood propagation has been considered, empirical studies [30] show their limited effectiveness in weakly supervised settings. Furthermore, research [5] establishes a relationship between aggregation-based models and random walks, revealing that as the number of layers increases, these models converge to the limit distribution of random walks, a property of the entire graph. Consequently, their performance deteriorates significantly with a high number of layers in weakly supervised settings.

In light of these challenges, we conduct a theoretical analysis that unveils the learning process of aggregation-based models as a seek for propagation operators of pairwise entity similarities. Based on this insight, we establish a key theoretical result: *potentially aligned entities in aggregation-based EA models possess isomorphic subgraphs, enabling the propagation of neighborhood information through these isomorphic subgraphs*. For example, as shown in Fig 1 right, potentially aligned entities (B,b) share isomorphic subgraphs enabling the propagation of neighborhood information through these isomorphic subgraphs. Leveraging this insight, we introduce **Potential isomorphism propagation Entity Alignment (PipEA)**, a general aggregation-based EA framework specifically designed to bridge the propagation gap in weakly supervised settings. PipEA constructs a propagation operator with two components: intra-graph propagation based on the original single-graph connectivity and inter-graph propagation grounded in potential alignment results represented by similarity matrices. This operator facilitates the generation of a new similarity matrix. We further propose a refinement scheme to better fuse the new and original similarity matrix. To reduce the complexity, we adopt randomized low-rank SVD [7] and the sinkhorn operator [3]. Extensive experiments demonstrate PipEA’s effectiveness, not only in weakly supervised settings but also in some normal supervised scenarios. In particular, our framework even improves the most dominant metric Hit@1 by

nearly two times compared to the original model and also achieves state-of-the-art on both cross-lingual and mono-lingual datasets.

Our main contributions are summarized as follows:

- **Theoretical Analysis:** We perform a theoretical analysis of aggregation-based EA models, illustrating their operation in terms of information propagation. Our analysis reveals that these models inherently seek propagation operators governing pairwise entity similarities. Furthermore, we establish that potentially aligned entities within these models exhibit isomorphic subgraphs, forming the theoretical foundation for our method.
- **Innovative Method:** We introduce PipEA, a theoretically grounded method designed to address the propagation gap prevalent in weakly supervised scenarios. To the best of our knowledge, PipEA is the first method capable of facilitating neighborhood information propagation between potentially aligned entities across heterogeneous graphs.
- **Extensive Experiments:** Experimental results validate our theoretical analysis and indicate our method achieves state-of-the-art on real-world datasets.

2 PRELIMINARY

2.1 Problem Definition

Definition 2.1. A *knowledge graph*, denoted as $\mathcal{G} = (\mathcal{E}, \mathcal{R}, \mathcal{T})$, comprises a set of entities \mathcal{E} , a set of relations \mathcal{R} , and a set of triples $\mathcal{T} = \{(h, r, t) \mid h, t \in \mathcal{E}, r \in \mathcal{R}\}$. Each triple represents an edge from the head entity h to the tail entity t with the relation r .

Definition 2.2. EA task aims to discover a one-to-one mapping of entities Φ from a source KG $\mathcal{G}_s = (\mathcal{E}_s, \mathcal{R}_s, \mathcal{T}_s)$ to a target KG $\mathcal{G}_t = (\mathcal{E}_t, \mathcal{R}_t, \mathcal{T}_t)$. Formally, seed alignment is denoted as $\Phi = \{(e_s, e_t) \mid e_s \in \mathcal{E}_s, e_t \in \mathcal{E}_t, e_s \equiv e_t\}$, where \equiv represents an equivalence relation between e_s and e_t .

2.2 Related Work

Aggregation-based EA. The adoption of aggregation-based models, featuring graph neural networks (GNNs), has gained significant traction in the domain of EA [33, 34, 40]. These models harness the power of GNNs to generate entity representations by aggregating information from neighboring entities [40]. Diverse GNN-based variants, such as RDGCN [39], RNM [49], KEGCN [10], MRAEA [19], and RREA [20], have emerged to address the capture of structural information and neighborhood heterogeneity. Some of these models focus on optimizing the proximity of positive entity pairs (e.g., PSR [17], Dual-AMN [18]) or the distance between negative pairs (e.g., SEA [22], TEA [14]). Furthermore, attribute-enhanced techniques incorporate entity attributes such as names and textual descriptions [15, 31, 42] to enhance entity embeddings. Notably, ACK [12] constructs an attribute-consistent graph to mitigate contextual gaps. Our work contributes by shedding light on these models’ underlying principles, revealing their quest for pairwise similarity propagation operators, and justifying the existence of isomorphic subgraphs within potentially aligned entities. Additionally, we introduce a novel general framework designed to augment the performance of these aggregation-based models.

Weakly Supervised EA. In scenarios with limited labeled data, many EA models suffer a drastic decline in alignment accuracy [37, 48]. Existing weakly supervised models, including ALEA [1], ActiveEA [13], RCL [46], and PEEA [30], primarily address the challenge of enhancing model generalization during the learning process. However, these methods often overlook the fundamental limitations of the original models when applied in weakly supervised settings. To bridge this gap, our method takes a novel perspective, analyzing the weakly supervised EA problem from the perspective of information propagation. It offers an effective enhancement method without altering the underlying model, thereby complementing existing weakly supervised EA methods.

3 THEORETICAL ANALYSIS

We delve into basic aggregation-based models and introduce propagation operators. Then we prove that potentially aligned entities have isomorphic subgraphs and design a new method based on it.

3.1 Aggregation-based EA

In aggregation-based EA models, entities are initially represented by aggregating their neighbors in the unified space. For simplicity, we consider a one-layer GCN [9] with mean-pooling as the aggregation function. The entity embedding in GCNs and the primary objective of alignment learning can be expressed as follows:

$$\mathbf{e} = \frac{1}{|N(e)|} \sum_{e' \in N(e)} \mathbf{e}' \quad (1)$$

$$\min_{(\mathbf{e}_s, \mathbf{e}_t) \in \Phi} d(\mathbf{e}_s, \mathbf{e}_t) \quad (2)$$

where $d(\cdot)$ represents a distance measure. The objective is to minimize the embedding distance between identical entities in seed alignments. While negative sampling methods aim to generate dissimilar entity pairs and train to distinguish the embeddings of dissimilar entities, Eq. 2 is the fundamental and commonly employed learning objective, which is the focus of our analysis.

3.2 Propagation Operators

The propagation operator is the core of propagation algorithms, governing information or influence spread in graphs. It is represented as a matrix or mathematical function. In general, propagation algorithms can be expressed as:

$$\pi_u(v) = \pi_u(v)P \quad (3)$$

π is used to signify the transition probability between nodes. One example is personalized PageRank (PPR) [21], where the propagation operator \hat{P} often takes the form $\hat{P} = D^{-1}A$. Here, D is a diagonal matrix, with $D(i, j)$ representing node i 's out-degree (for directed) or degree (for undirected graphs), and A is the adjacency matrix. PPR $\pi_u(v)$ for node v regarding node u quantifies the probability of a random walk with an α discount initiated from u ending at v , with α denoting the probability of stopping at the current node and $(1 - \alpha)$ the probability of transitioning to a random out-neighbor. PPR propagation can be expressed as:

$$\pi_{PPR} = \sum_{\ell=0}^{\infty} \alpha(1 - \alpha)^\ell \hat{P}^\ell \quad (4)$$

3.3 Analysis of Aggregation-based EA

The Aggregation-based EA model is commonly evaluated on heterogeneous graphs [4, 11, 29, 41]. Entity similarities are computed using embeddings from aggregation-based models, denoted as (x_1, x_2, \dots, x_n) and (y_1, y_2, \dots, y_m) , with $n = |\mathcal{E}_s|$ and $m = |\mathcal{E}_t|$. The pairwise similarity matrix, crucial for entity alignment, is defined as:

$$\Omega = (x_1; x_2; \dots; x_n)^\top (y_1; y_2; \dots; y_m) \in \mathbb{R}^{n \times m} \quad (5)$$

Similar to most EA settings, we assume that each entity aligns with at most one entity in another KG.

Proposition 3.1. *In the Aggregation-based EA model, the primary objective is to derive a propagation operator governing pairwise entity similarities via embedding learning.*

PROOF. Please refer to Appendix.A.1 \square

This proposition clarifies that the Aggregation-based EA model seeks a propagation operator operating on the similarity matrix. Recent studies employ such kind operators on proximity matrices [43, 44, 47], representing entity proximity within a single graph. Proposition 3.1 suggests that the similarity matrix can also be seen as a specialized proximity matrix, where $\Omega(i, j)$ measures the proximity between node i and node j in another graph within a unified space. This implies that $\Omega(i, j)$ captures potential structural information between cross-graph entities in the unified space. Moreover, the propagation operator derived from the learning process unveils the structure of subgraphs for potentially aligned entity pairs within this unified space. Therefore, we provide the following proposition.

Proposition 3.2. *Let $\Lambda = [\lambda_1, \dots, \lambda_n] \in \mathbb{R}^{n \times n}$ represent a matrix comprising n arbitrary orthonormal vectors, signifying the propagation operator derived from aggregation-based EA models. Then potentially aligned entities have isomorphic subgraphs, and it follows that $Pr(\text{rank}(\Lambda\Lambda^\top) = n) = 1$.*

PROOF. Please refer to Appendix.A.2 \square

3.4 Potential Isomorphism Propagation

Entities communicate through information propagation, facilitated by isomorphic subgraphs and graph connectivity [8]. Traditionally, this process was confined to individual graphs due to heterogeneity and varying intra-graph connectivity. However, Proposition 3.2 in the Aggregation-based EA model establishes that potentially aligned entities indeed share isomorphic subgraphs, a property inherently reflected in the similarity matrix. This leads us to propose *Potential Isomorphism Propagation*. This concept harnesses the unified space's similarity matrix to control information propagation between potentially aligned entities with isomorphic subgraphs. To implement this idea, we introduce a propagation operator containing inter-graph and intra-graph propagation, and its effectiveness is formally proven. In this model, information flow between potentially aligned entities is governed by the similarity matrix, while intra-graph propagation relies on the graph's connectivity represented as $D^{-1}A$. Let D_γ and A_γ denote the degree matrix and adjacency matrix for \mathcal{G}_γ , where $\gamma = \{s, t\}$.

Proposition 3.3. *Let $\Lambda_1 = [D_s^{-1}A_s, \Omega] \in \mathbb{R}^{n \times (n+m)}$, $\Lambda_2 = [\Omega^\top, D_t^{-1}A_t] \in \mathbb{R}^{m \times (n+m)}$, and $\hat{\Lambda} = [\Lambda_1; \Lambda_2] \in \mathbb{R}^{(n+m) \times (n+m)}$.*

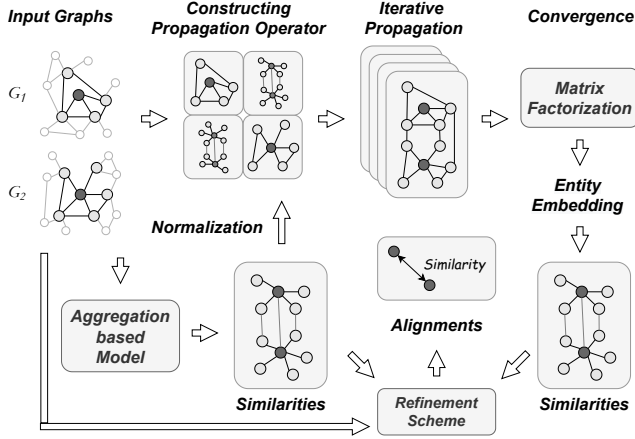


Figure 2: PipEA starts with initial pairwise similarities from aggregation-based models. We construct a propagation operator and apply matrix factorization to derive new entity embeddings. A refinement scheme is then introduced to effectively integrate various pairwise similarities.

Consider $\hat{\Lambda} \in \mathbb{R}^{(n+m) \times (n+m)}$ as a symmetric graph operator with $\lambda_1, \dots, \lambda_d$ as its d dominant eigenvalues (in decreasing order of magnitude), where $|\lambda_i| > |\lambda_{i+1}|$, $1 \leq i \leq d$. Then, the Potential Isomorphism Propagation strategy, $\hat{\Lambda}\hat{\Lambda}^\top$, converges to the d -dominant eigenvectors.

PROOF. Please refer to Appendix.A.3 \square

4 METHOD

PipEA introduces a novel approach to enhance weakly supervised EA by leveraging potential isomorphism, as detailed in Section 1. This section outlines PipEA’s framework, grounded in the principles established in Proposition 3.3.

4.1 Overview of the Framework

PipEA unfolds in several phases, starting with an initial similarity matrix Ω_0 produced by an aggregation-based EA model, as illustrated in Fig. 2. The core of PipEA is isomorphism propagation, which advances information sharing across KGs through a sequence of steps: *constructing the propagation operator*, *iterative propagation*, *matrix factorization*, and *refinement scheme*.

Matrix factorization yields new entity embeddings, enabling the creation of a refined similarity matrix. This new matrix surpasses the initial one by capturing both local and cross-graph structural similarities, thanks to the GNN layers that encode neighborhood information. The propagation operator thus facilitates linking entities in distinct graphs with analogous local structures.

Our refinement scheme enhances this process by integrating the newly derived similarity matrix with the initial one, further refined through a multiplication operation. An advanced refinement scheme is also introduced to ensure neighborhood consistency within each graph, thus maintaining the integrity of subgraph structures in the unified space.

In this paper, we utilize two leading EA models, DualAMN [18] and PEEA [30], to generate Ω_0 . DualAMN, the state-of-the-art (SOTA) in normal supervised EA, employs proxy matching and hard negative sampling with GCNs. PEEA, SOTA in weakly supervised EA, leverages anchor positioning for dependency mapping and has shown exemplary performance among structure-only aggregation-based EA methods. The encoding process is formalized as:

$$\Omega_0 = \text{Encoder}(A_s, A_t) \quad (6)$$

The implementation details of PipEA are provided in Algorithm 1.

4.2 Isomorphism Propagation

4.2.1 Constructing the Propagation Operator. Our propagation operator combines intra-graph and inter-graph propagation. Intra-graph propagation is based on the normalized adjacency matrix $D^{-1}A$ of the single-graph structure, while inter-graph propagation uses the similarity matrix $\Omega \in \mathbb{R}^{n \times m}$. The operator is defined as:

$$\hat{\Lambda} = \begin{bmatrix} \beta \cdot D_s^{-1}A_s & (1 - \beta) \cdot \mathcal{N}^{l_2}(\Omega_0) \\ (1 - \beta) \cdot \mathcal{N}^{l_2}(\Omega_0^\top) & \beta \cdot D_t^{-1}A_t \end{bmatrix} \in \mathbb{R}^{(n+m) \times (n+m)} \quad (7)$$

Here, the parameter β balances intra-graph and inter-graph propagation. Notably, we focus on similarities between highly confident potentially aligned pairs using a normalization operation denoted as $\mathcal{N}^{l_2}(\cdot)$, which is applied on rows as follows:

$$\mathcal{N}^{l_2}(\Omega(i, :)) = \frac{\varphi_k(\Omega(i, :))}{\|\varphi_k(\Omega(i, :))\|_2} \quad (8)$$

where φ_k denotes a ranking scheme that preserves the top k candidates ($\omega_1^c, \dots, \omega_k^c$) and sets others to zero.

$$\mathcal{N}^{l_2}(\Omega(i, :)) = [0, \dots, \omega_1^c, \dots, 0, \dots, \omega_k^c, \dots, 0] \in \mathbb{R}^m \quad (9)$$

It’s worth noting that for any $(e_j, e_{j'}) \in \Phi$ within the seed alignments, inter-graph propagation exclusively occurs between the aligned entity pairs, and their $\mathcal{N}^{l_2}(\Omega(j, :))$ is precisely defined as a vector with only one nonzero value at the j' -th element:

$$\mathcal{N}^{l_2}(\Omega(j, :)) = \mathbb{I}_{j'} = [0, \dots, 1, \dots, 0] \in \mathbb{R}^m \quad (10)$$

4.2.2 Propagation Strategy. Inspired by the PPR formulation in Eq. 3, we introduce a random-walk propagation method to harness the potential isomorphism phenomenon, denoted as:

$$S = \sum_{\ell=0}^{\infty} \alpha(1 - \alpha)^\ell \hat{\Lambda}^\ell \quad (11)$$

This method facilitates the propagation of neighborhood information through isomorphic subgraphs between potentially aligned entities.

4.2.3 Matrix Factorization. In experiments, we observed that matrix S eliminates small values. To adapt for large-scale datasets, we introduce a threshold δ where values below it are set to zero. Then, we compute $\log(\frac{S}{\delta})$ for non-zero entries, obtaining a sparse matrix approximating the propagation results.

Next, using a differentiable Singular Value Decomposition (SVD) [7] with input dimension d , we factorize the matrix S . This produces U and V matrices, both of size $(n + m) \times d$, along with a diagonal matrix Σ , such that $U\Sigma V^\top \approx S$:

$$U, \Sigma, V^\top = \text{SVD}(\text{Sparse}(S, \delta), d) \quad (12)$$

Finally, we compute entity embeddings X as:

$$X = U\sqrt{\Sigma} \quad (13)$$

This method ensures robust and informative information propagation within the unified space. Subsequently, we derive global pairwise similarities by using source embeddings $X_s = X[:n]$ and target embeddings $X_t = X[n:n+m]$:

$$\Omega'_0 = X_s X_t^\top \quad (14)$$

4.2.4 Refinement Scheme. Two similarity matrices are generated in the previous process. The first is the initial similarity matrix produced by the aggregation-based EA model, emphasizing local information via n-hop neighborhood aggregation. The second is the propagation scheme, which focuses on global information in the unified space. To integrate these matrices, we employ element-wise Hadamard products, resulting in a new matrix denoted as $\bar{\Omega}_0$:

$$\bar{\Omega}_0 = \Omega_0 \circ \Omega'_0 \quad (15)$$

However, the direct fusion of these matrices can potentially compromise topological consistency information within the original similarity matrices. [4]. To mitigate this loss, we introduce a refinement scheme that centers on preserving topological consistency. This refinement scheme leverages the concept of matched neighborhood consistency (MNC) scores [6] to quantify topological consistency and iteratively enhances these scores.

The MNC score was originally defined as:

$$S^{MNC} = A_s \Omega A_t \oslash (A_s \Omega 1^m \otimes 1^m + 1^n A_t 1^m - A_s \Omega A_t) \quad (16)$$

Here, \oslash denotes element-wise division, and \otimes signifies the Kronecker product. However, for simplification purposes, we approximate it as follows:

$$S^{MNC} \approx A_s \Omega A_t \quad (17)$$

To iteratively update the similarity matrix $\bar{\Omega}$ in the k -th iteration, we introduce a small ϵ to every element of $\bar{\Omega}$ to assign every pair of nodes a token match score, irrespective of whether the initial EA model identified them as matches. This enables us to rectify potential false negatives present in the initial similarity matrix. The similarities for aligned entity pairs are set as a one-nonzero-value vector, as illustrated in Eq. 19:

$$\bar{\Omega}_k = \phi(\bar{\Omega}_{k-1} \circ A_s \bar{\Omega}_{k-1} A_t + \epsilon) \quad (18)$$

Here, the function ϕ selects the entity pairs from the seed alignments Φ and assigns them a similarity score of 1, while setting all other values to zero. It is defined as:

$$\phi(\Omega, (e_i, e_j) \in \Phi) := \Omega(i) = \mathbb{I}_j = [0, \dots, 1, \dots, 0] \quad (19)$$

This iterative refinement process is a critical component of our PipEA method, enabling the correction of potential biases and enhancing the alignment accuracy.

Remark: The refinement Scheme is distinct from RefiNA [6]. While RefiNA is an unsupervised graph matching technique, our scheme is supervised which introduces dynamic influence on the MNC score in each iteration through seed alignments.

Algorithm 1 Potential Isomorphism Propagation Strategy

Input:

The adjacency matrices A_s, A_t , number of iterations L_1, L_2 , embedding dimension d , seed alignments Φ

Output:

The final refined similarity matrix $\bar{\Omega}$.

- 1: Initialize $S = \mathbf{0}, R = \mathbf{I}$. (\mathbf{I} is the identity matrix)
 - 2: $\Omega_0 \leftarrow \text{Encoder}(A_s, X_t)$
 - 3: Constructing the propagation operator $\hat{\Lambda}$.
 - 4: **for** $k = 1 \rightarrow L_1$ **do**
 - 5: $S \leftarrow S + \alpha \cdot R$
 - 6: $R \leftarrow S + (1 - \alpha) \cdot \hat{\Lambda} \cdot R$
 - 7: **end for**
 - 8: **for** $\forall S(i, j) \in S$ **do**
 - 9: **if** $S(i, j) < \delta$, **then** $S(i, j) \leftarrow 0$
 - 10: **end for**
 - 11: Get matrix $\log(\frac{S}{\delta})$ for non-zero entries
 - 12: $[U, \Sigma, V^\top] \leftarrow \text{Differentiable Sparse SVD}(\log(\frac{S}{\delta}), d)$
 - 13: Get the eigenvector entity embedding matrix $X \leftarrow U\sqrt{\Sigma}$
 - 14: $\bar{\Omega}' \leftarrow X_s X_t^\top$
 - 15: $\bar{\Omega}_0 \leftarrow \Omega_0 \circ \bar{\Omega}'$
 - 16: **for** $k = 1 \rightarrow L_2$ **do**
 - 17: $\bar{\Omega}_{k-1} \leftarrow \phi(\bar{\Omega}_{k-1}, \Phi)$
 - 18: $\bar{\Omega}_k \leftarrow \bar{\Omega}_{k-1} \circ A_s \bar{\Omega}_{k-1} A_t + \epsilon$
 - 19: $\bar{\Omega}_k \leftarrow \text{Normalize } \bar{\Omega}_k \text{ by row then column}$
 - 20: **end for**
 - 21: **return** $\bar{\Omega}$
-

4.3 Reducing Time Complexity

The PipEA method introduces potential isomorphism propagation to intricately map the inter- and intra-structural nuances of KGs. Despite its comprehensive approach, this technique inherently increases time complexity, primarily due to the computation of $S \in \mathbb{R}^{(n+m) \times (n+m)}$. To mitigate this, we employ strategies to streamline the computational process:

4.3.1 Sparse threshold. Referenced in Section 4.2.3, a sparse threshold δ is applied, setting all scores below δ to zero. This approach filters out insignificant entities, focusing on those most likely to contribute to accurate propagation outcomes. An in-depth analysis of the impact of δ is presented in our experimental section.

4.3.2 Low-rank SVD. Following observations by [16, 36] that significant information in S is concentrated in the top singular values, we employ randomized low-rank SVD [7]. This method approximates matrix decomposition, retaining only the top 1% of singular values, thus reducing both space and time complexity.

4.3.3 Sinkhorn operator. Traditional EA methodologies calculate entity pair similarities directly, leading to potential violations of the one-to-one alignment constraint. To circumvent this, the transformation of the EA decoding process into an assignment problem has shown promise [16, 30], markedly improving performance:

$$\arg \max_{\mathbf{P} \in \mathbb{P}_{|E|}} \langle \mathbf{P}, \Omega \rangle_F \quad (20)$$

Table 1: Main results of cross-lingual and mono-lingual datasets. underline means the best existing models. PEEA is the SOTA of weakly supervised EA and DualAMN is the SOTA of normal supervised EA. "Improv." represents the percentage increase compared with the original model. PipEA(P) means PEEA is the encoder and PipEA(D) means DualAMN is the encoder.

Datasets	Cross-Lingual Datasets									Mono-Lingual Datasets										
	15KEN-DE			15KEN-FR			100KEN-FR			15KDBP-Wiki			15KDBP-Yago			100KDBP-Wiki				
Models	H@1	H@10	MRR	H@1	H@10	MRR	H@1	H@10	MRR	H@1	H@10	MRR	H@1	H@10	MRR	H@1	H@10	MRR		
Basic	GCN-Align	10.9	26.7	16.4	3.6	15.2	7.1	2.5	9.4	5.0	3.1	11.0	5.8	40.1	60.6	47.1	3.5	11.4	6.2	
	PSR	21.5	49.7	31.0	15.1	38.1	22.9	13.2	32.9	19.9	19.5	44.2	27.9	25.3	51.6	34.2	14.6	33.5	21.0	
	MRAEA	28.6	58.7	38.7	14.4	38.5	22.4	13.5	36.1	21.0	19.4	45.4	28.1	42.9	72.4	53.1	17.1	39.7	24.7	
	RREA	48.5	72.5	56.8	26.3	56.4	36.4	16.4	40.6	24.5	41.8	67.5	50.7	82.1	92.8	86.0	21.4	45.9	29.7	
	DualAMN	51.9	75.4	60.1	25.2	52.1	34.3	15.0	38.6	22.8	40.0	64.5	48.5	76.2	88.3	80.7	16.2	37.7	23.5	
	PipEA(D)	82.3	86.4	83.9	48.5	58.9	52.4	36.8	64.6	46.6	71.6	76.3	73.4	96.7	97.8	97.2	31.9	54.6	39.6	
	Improv.	58.6%	14.6%	39.6%	92.5%	13.1%	52.8%	145.3%	67.3%	104.4%	79.0%	18.3%	51.3%	26.9%	10.8%	20.4%	96.9%	44.8%	68.5%	
	PEEA	68.6	88.1	75.4	44.0	72.4	53.6	20.3	47.6	29.4	59.4	81.2	67.1	92.6	97.4	94.4	24.4	50.6	33.2	
	PipEA(P)	85.4	92.0	87.8	58.1	74.4	63.7	49.6	54.0	38.5	75.4	82.5	77.9	96.9	98.4	97.5	37.2	58.5	44.3	
	Improv.	24.5%	4.4%	16.4%	32.0%	2.8%	18.8%	144.3%	13.4%	31.0%	26.9%	1.6%	16.1%	4.6%	1.0%	3.3%	52.5%	15.6%	33.4%	
	Iterative	BootEA	0.6	3.6	1.7	2.7	10.1	5.2	2.1	4.4	5.4	1.8	7.4	3.7	2.7	1.6	6.6	3.3	40.5	28.2
		KECG	42.5	64.6	50.2	14.1	43.3	23.7	11.1	30.5	17.7	23.8	45.8	31.3	57.8	78.8	65.1	20.2	42.4	27.8
		SEA	43.1	66.5	51.2	18.9	49.4	29.1	12.5	34.5	19.9	15.6	40.4	24.0	81.4	92.7	85.5	13.6	33.6	20.4
		PSR	79.9	91.4	84.1	52.8	75.3	60.5	55.4	72.6	62.0	72.1	85.5	77.1	95.2	97.9	96.3	59.3	68.4	61.7
		MRAEA	64.7	84.5	72.3	35.9	61.7	44.7	38.2	64.1	55.1	58.6	78.4	66.5	88.5	97.8	92.7	45.8	60.2	48.4
RREA		76.5	90.7	81.8	39.6	68.0	49.5	55.2	74.1	63.3	66.8	83.5	73.1	95.6	98.3	96.7	58.0	71.8	62.7	
Dual-AMN		77.1	93.0	83.6	48.4	79.0	59.4	57.3	76.2	65.9	67.2	86.6	75.1	92.4	98.4	95.2	59.6	72.1	63.8	
PipEA(D)		86.6	93.5	88.1	61.3	70.6	64.9	67.7	84.9	73.3	78.4	82.5	80.0	97.0	98.5	97.6	71.8	70.6	68.1	
Improv.		12.26%	0.52%	5.41%	26.74%	-	9.33%	18.15%	11.40%	11.29%	16.61%	-	6.48%	1.56%	0.1%	0.89%	20.45%	-	6.68%	
PEEA		83.6	93.2	87.1	55.6	79.4	64.0	59.6	77.6	66.3	78.5	90.0	82.7	96.6	98.6	97.3	65.3	78.2	70.6	
PipEA(P)		90.7	95.4	92.5	80.1	89.8	83.6	71.6	86.1	76.7	84.3	90.9	86.1	97.2	98.9	97.7	77.6	86.8	80.8	
Improv.		8.5%	2.4%	6.2%	44.1%	13.1%	30.6%	20.1%	11.0%	15.7%	7.4%	1.0%	4.1%	0.6%	0.3%	0.4%	18.8%	11.0%	14.4%	

Here, Ω denotes the similarity matrix, and P is a permutation matrix that outlines the alignment strategy. While the Hungarian algorithm offers a precise solution, its $O(|\mathcal{E}|^3)$ complexity is prohibitive for large KGs. Adopting the Sinkhorn operator [3], we apply a scalable and parallelizable algorithm, significantly reducing the computational load to $O(q|\mathcal{E}|^2)$ with q set to 10 iterations. The details of the Sinkhorn are listed in Appendix.

5 EXPERIMENTS

In this section, we conduct a rigorous evaluation of our PipEA method on real-world datasets, benchmarking its performance against state-of-the-art (SOTA) EA models. We introduce our experimental settings and present detailed results below.

5.1 Experimental Settings

5.1.1 Datasets. To assess PipEA’s effectiveness, we turn to the OpenEA benchmark dataset (V2), thoughtfully designed to closely mirror the data distribution found in real knowledge graphs. Our evaluation encompasses two cross-lingual settings (English-to-French and English-to-German), sourced from the multilingual DBpedia, and two monolingual settings (DBpedia-to-Wikidata and DBpedia-to-YAGO), extracted from popular knowledge bases. In each setting, we consider two sizes: one with 15K pairs of reference entities and another with 100K pairs. In contrast to the conventional use of 30%

of seed alignments for training, we adopt weakly supervised scenarios, employing only 1% of seed alignments randomly sampled from the datasets. For more details, please refer to Appendix D.

5.1.2 Evaluation Metrics. Performance assessment is based on the official Mean Reciprocal Rank (MRR), H@1, and H@10 metrics, widely recognized and embraced in EA studies. Elevated H@1, H@10, and MRR scores signify superior EA performance. Our default alignment direction is from left to right (e.g., EN as the source KG and FR as the target KG for the EN-FR dataset).

5.1.3 Baselines. We compare our PipEA with 9 prominent methods that solely rely on the original structure information, divided into two groups:

- Basic models: GCN-Align [38], MRAEA [19], RREA [20], PSR [17], Dual-AMN [18] and PEEA [30].
- Iterative strategy: The *iterative training strategy* is also applied for the basic models to improve their performance and further evaluate the ability of PipEA. In addition to the basic models described above, we have added a model that specializes in iterative processing such as BootEA [27], KECG [10], SEA [22].

We adhere to the default hyper-parameters as reported in their respective literature.

5.1.4 Iterative training strategy. After training the base model with fundamental settings, in every epoch K_e (in our paper $K_e = 10$), cross-KG entity pairs that are mutual nearest neighbors in the vector space are proposed and added to a candidate list N^{cd} . An entity pair in N^{cd} is incorporated into the training set if it remains a mutual nearest neighbor for K_c consecutive rounds (where $K_c = 10$).

5.1.5 Parameter Settings. Following previous studies [23, 32, 44], we set the embedding dimensionality to $d = 128$ and determine the token match score $\epsilon = 0.00001$. We employ 8 propagation and refinement iterations ($L_1 = 8$ and $L_2 = 8$) in experiments. For further insights into hyper-parameters, kindly refer to Section 5.5 and Appendix E.

5.1.6 Computational Resources. All experiments were diligently executed on a server equipped with an NVIDIA A100 and NVIDIA A800 GPU. A comprehensive analysis of the computational complexity of our method is thoughtfully detailed in Appendix C.

5.2 Main Results

Our evaluation of PipEA across six cross-lingual and monolingual datasets, under the condition of 1% seed alignments, is summarized in Table 1. The results lead to several key insights:

(1) PipEA significantly surpasses standard alignment models using various encoders in both cross-lingual and monolingual contexts. Notably, on the 100K EN-FR datasets, it records substantial increases of 145.3% and 144.3% in the H@1 metric for PEEA and DualAMN, respectively. These outcomes confirm that (i) isomorphic subgraphs among potentially aligned entities facilitate robust information propagation, and (ii) our propagation approach effectively leverages this characteristic in a unified embedding space.

(2) In terms of Mean Reciprocal Rank (MRR), PipEA demonstrates enhancements from 20.4% to 52.8% on 15K datasets and from 68.5% to 104.4% on 100K datasets, underscoring its adaptability and effectiveness across different dataset sizes. These results underscore PipEA’s capacity to substantially elevate the performance of existing models in weakly supervised scenarios, making it a superior option for weakly supervised entity alignment tasks.

(3) It is evident that the iterative strategy significantly enhances entity alignment by iteratively incorporating high-quality aligned entity pairs into the training data to refine the model. Specifically, PipEA demonstrates remarkable improvements of 17.3% and 9.4% accuracy on 15K EN-FR and 100K DBP-Wiki datasets. In terms of H@1 and MRR, improvements are observed across various datasets. Notably, even without the iterative strategy, PipEA surpasses most iterative models on all 15K datasets, and on the 15K DBP-Wiki dataset, it outperforms LightEA (Iter.). This exceptional performance underscores the effectiveness of our method in identifying high-quality aligned entity pairs for iterative training.

(4) PipEA consistently outperforms existing weakly supervised aligners across all datasets. While these methods employ techniques to enhance accuracy, they primarily propagate neighborhoods within individual graphs. As discussed in Section 1, the key challenge in weakly supervised EA is limited neighborhood propagation on the graph. We find that potentially aligned entities indeed possess isomorphic subgraphs capable of propagating neighborhoods. PipEA, with its cross-graph propagation operator,

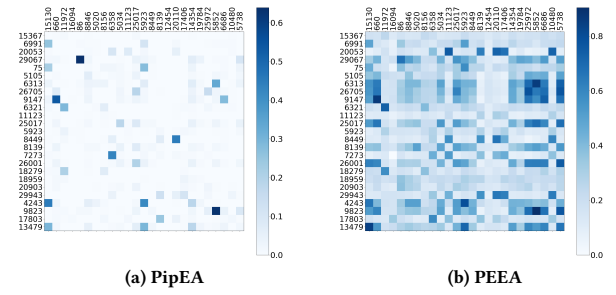


Figure 3: Similarity matrix of our method and SOTA encoder on sub-graph from 15KEN-DE.

Table 2: H@1 of different methods without iterative strategy under different supervised settings. PEEA is the encoder.

Dataset	15KEN-DE					15KEN-FR				
	1%	5%	10%	20%	30%	1%	5%	10%	20%	30%
Seed Ratio										
Ours	85.4	90.64	92.47	94.62	95.46	58.12	79.87	83.56	88.07	90.24
PEEA	68.67	84.58	91.13	94.75	95.94	44.07	68.73	77.4	84.88	90.04
RREA	48.5	76.1	83.44	88.74	90.53	26.23	55.64	68.64	78.2	81.91
Dual-AMN	51.95	76.46	86.13	91.2	93.17	25.28	55.51	68.11	78.78	84.11
MRAEA	28.63	68.56	81.42	88.1	90.72	14.42	45.82	61.75	73.82	79.76
PSR	21.59	62.17	76.83	85.61	89.09	15.18	45.81	60.69	73.06	79.66
GCN-Align	10.99	20.76	24.21	27.43	30.5	3.68	12.84	18.76	23.52	28.83

successfully bridges this gap by facilitating neighborhood propagation between potentially aligned entities in different graphs, resulting in improved alignment accuracy.

(5) Our case study analysis, focused on the 15KEN-DE dataset, examines the pairwise similarity quality between SOTA models and PipEA. By analyzing a subgraph of 25 entities, we visualized the similarity matrices of PipEA and PEEA through heat maps (Fig.3). PipEA exhibits markedly clearer and more distinct similarity distributions than PEEA, underscoring its superior ability to refine similarity matrices for accurate entity pair identification. This clarity in similarity distribution explains PipEA’s improved H@1 performance contrasted with H@10 performance, indicating its effectiveness in establishing confident one-to-one alignments without necessitating an extensive candidate pool.

5.3 Discussions for Supervised Settings

To assess the generality of our method under different supervised settings, we conducted comprehensive experiments comparing PipEA with baseline methods at different training data ratios (1%, 5%, 10%, 20%, and 30%) using the 15KEN-DE and 15KEN-FR datasets. The results summarized in Table 2 reveal several key insights: (1) Our method demonstrates remarkable performance even in conventional supervised settings. While its advantage over other baselines may diminish as the training ratio increases, PipEA consistently outperforms them. Notably, it achieves superior performance compared to baselines on the 15K EN-FR dataset, even when the seed

Table 3: Ablation experiments without the iterative training strategy on cross-lingual and mono-lingual datasets

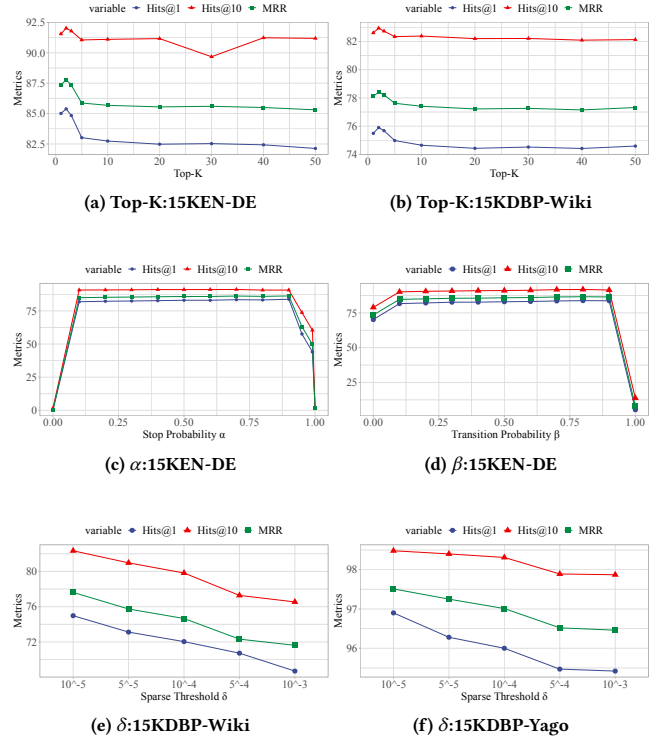
Methods	15KEN-DE			15KEN-FR		
	H@1	H@10	MRR	H@1	H@10	MRR
Ours	85.40	92.03	87.80	58.12	74.42	63.69
w/o RS	79.99	91.24	81.24	49.72	72.72	58.95
w/o IS	78.48	88.84	81.98	48.27	70.4	55.53
w/o PS	75.64	88.06	79.92	49.53	70.18	56.52

Methods	15KDBP-Yago			15KDBP-Wiki		
	H@1	H@10	MRR	H@1	H@10	MRR
Ours	96.90	98.48	97.51	75.40	82.55	77.94
w/o RS	95.32	98.2	96.47	69.89	81.57	74.51
w/o IS	92.46	96.63	93.95	67.93	77.49	71.08
w/o PS	92.32	97.99	94.43	67.36	82.72	73.07

alignment ratio is as high as 30%. This phenomenon can be attributed to the nature of aggregation-based EA models, which operate by propagating neighborhood information. PipEA’s unique capability to propagate information across graphs extends the size of the neighborhood involved in this propagation process, contributing to its sustained success across varying degrees of supervision. (2) The performance gap between PipEA and baselines in weakly supervised scenarios gradually narrows as the training ratio increases. The alignment performance on the 15K EN-DE dataset is lower than PEEA [30] when the seed alignment ratio exceeds 10%. This is because the propagation gap is diminished with substantial seed alignments available and PipEA was originally designed to tackle the challenges of limited seed alignments.

5.4 Ablation Study

To comprehensively evaluate the contributions of each component within PipEA, we conducted an ablation study based on PEEA encoder, introducing three variants of the model, as presented in Table 3: (1) w/o RS (Refinement Scheme): In this variant, we excluded the refinement scheme, directly multiplying the initial similarity matrix Ω_0 with the generated similarity matrix Ω'_0 . As discussed in Section 4.2.4, directly fusing different similarity matrices can result in a loss of topological consistency information. Compared to our complete PipEA method, w/o RS led to a reduction in MRR ranging from 1.04% to 6.56% on the 15K datasets. Notably, the H@1 exhibited a significant drop of 8.4% on 15K EN-FR. This suggests that without the refinement scheme, the model may produce more erroneous predictions, especially when only one outcome can be predicted. (2) w/o IS (Initial Similarity): In this case, we excluded the initial similarity matrix Ω_0 and solely utilized Ω'_0 as the final similarity matrix. It is crucial to note that the initial similarity matrix generated by the aggregation-based EA model primarily captures local similarities arising from its n-hop neighborhood information aggregation. Conversely, our method provides global similarities. By removing these local similarities, we observed a notable decrease in model performance, ranging from 4.44% to 9.85% in terms of H@1. (3) w/o PS (Potential Isomorphism Propagation): In this variant, we omitted the generated similarity matrix Ω'_0 . These experiments offered insights into the effectiveness of potential isomorphism propagation. Across the 15K datasets, w/o PS resulted in a substantial reduction

**Figure 4: Hyper-parameter experiments of our method.**

in H@1, ranging from 4.58% to 9.76%. This outcome underscores the critical role of potential isomorphism propagation in our method. Furthermore, it highlights that our refinement scheme can effectively preserve topological consistency within the similarity matrix, leading to improved alignment accuracy.

5.5 Hyper-parameters

5.5.1 Top-K Selection. PipEA employs a parameter, denoted as k , to select potentially aligned entities for propagation through normalization operations. It is represented as ϕ_k in the normalization operations Eq.8. Fig. 4(a)(b) illustrates the sensitivity of alignment accuracy to the number of potentially aligned entities. Interestingly, our method achieves peak performance on both the EN-DE and DBP-Wiki datasets across all metrics when $k = 2$. Further increasing the value of k leads to diminishing accuracy, suggesting that allowing too many entities to share isomorphic subgraphs within the unified space may negatively impact performance. Consequently, we set $k = 2$ as the optimal choice for our study.

5.5.2 Random Walk Probability. The parameter α determines the probability of stopping at the current entity during a random walk. As depicted in Fig. 4(c), PipEA exhibits robust performance within the range of α from 0.1 to 0.9. The highest H@1 score (85.4%) is achieved at approximately $\alpha = 0.7$, which we adopt in our study. Notably, our experiments reveal that PipEA’s effectiveness is compromised under two extreme conditions: when $\alpha = 0$, indicating constant random walks among all entities across graphs, and when

$\alpha = 1$, signifying a lack of neighborhood information propagation. These findings empirically validate the effectiveness of our method.

5.5.3 Inter-Intra Graph Balance. Eq. 7 outlines the propagation operator, consisting of intra-graph and inter-graph propagation components, with β controlling the balance between these aspects. Specifically, β determines the probability of propagation occurring within the intra-graph part compared to the inter-graph part. Fig. 4(d) demonstrates that PipEA consistently performs well for β values ranging from 0.1 to 0.9. We set $\beta = 0.5$ in this work. Notably, when $\beta = 0$, signifying propagation solely across graphs, H@1 exhibits a slight degradation, affirming PipEA’s ability to capture neighborhood information in the unified space. Conversely, when $\beta = 1$, indicating exclusive intra-graph propagation, H@1 drops significantly (1.36%), underscoring the challenge of capturing entity dependencies between different graphs relying solely on single-graph structures. This emphasizes the rationale behind our method, which combines intra-graph and inter-graph propagation.

5.5.4 Threshold. To ensure the non-negativity of the generated matrix and its applicability across graphs of varying scales, we utilize the threshold δ , as outlined in Section 4.2. Our experiments indicate that accuracy declines as δ decreases, signifying the loss of valuable neighborhood information, as depicted in Fig. 4(e)(f). This reaffirms the effectiveness of PipEA on 100K datasets and its significant performance improvements compared to baseline methods.

6 CONCLUSION

This research addresses the challenges of weakly supervised EA characterized by limited seed alignments. Through a propagation perspective, we analyze how aggregation-based EA models utilize operators to propagate pairwise entity similarities. A key insight from our theoretical analysis is the existence of isomorphic subgraphs among potentially aligned entities, facilitating effective information propagation essential for EA tasks. We develop PipEA, a general and novel approach that synergizes intra-graph and inter-graph propagation techniques while refining similarity matrices to enhance alignment accuracy. Our experimental results affirm PipEA’s effectiveness, showcasing its superiority over state-of-the-art models in both weakly supervised and fully supervised contexts. PipEA thus serves as a pivotal step forward, reconciling recent advancements in aggregation-based EA with traditional propagation-based graph learning methodologies.

REFERENCES

- [1] Max Berrendorf, Evgeniy Faerman, and Volker Tresp. 2021. Active learning for entity alignment. In *Advances in Information Retrieval: 43rd European Conference on IR Research, ECIR 2021, Virtual Event, March 28–April 1, 2021, Proceedings, Part 1* 43. Springer, 48–62.
- [2] Soumen Chakrabarti. 2022. Deep knowledge graph representation learning for completion, alignment, and question answering. In *Proceedings of the 45th International ACM SIGIR Conference on Research and Development in Information Retrieval*. 3451–3454.
- [3] Marco Cuturi. 2013. Sinkhorn distances: Lightspeed computation of optimal transport. *Advances in neural information processing systems* 26 (2013).
- [4] Yunjun Gao, Xiaozhe Liu, Junyang Wu, Tianyi Li, Pengfei Wang, and Lu Chen. 2022. Clusterea: Scalable entity alignment with stochastic training and normalized mini-batch similarities. In *Proceedings of the 28th ACM SIGKDD Conference on Knowledge Discovery and Data Mining*. 421–431.
- [5] Johannes Gasteiger, Aleksandar Bojchevski, and Stephan Günnemann. 2018. Predict then Propagate: Graph Neural Networks meet Personalized PageRank. In *International Conference on Learning Representations*.
- [6] Mark Heimann, Xiyuan Chen, Fatemeh Vahedian, and Danai Koutra. 2021. Refining network alignment to improve matched neighborhood consistency. In *Proceedings of the 2021 SIAM International Conference on Data Mining (SDM)*. SIAM, 172–180.
- [7] Piotr Indyk, Ali Vakilian, and Yang Yuan. 2019. Learning-based low-rank approximations. *Advances in Neural Information Processing Systems* 32 (2019).
- [8] Tatsuhiro Kawamoto, Masashi Tsubaki, and Tomoyuki Obuchi. 2018. Mean-field theory of graph neural networks in graph partitioning. *Advances in Neural Information Processing Systems* 31 (2018).
- [9] Thomas N Kipf and Max Welling. 2016. Semi-Supervised Classification with Graph Convolutional Networks. In *International Conference on Learning Representations*.
- [10] Chengjiang Li, Yixin Cao, Lei Hou, Jiaxin Shi, Juanzi Li, and Tat-Seng Chua. 2019. Semi-supervised entity alignment via joint knowledge embedding model and cross-graph model. Association for Computational Linguistics.
- [11] Jia Li and Dandan Song. 2022. Uncertainty-aware pseudo label refinery for entity alignment. In *Proceedings of the ACM Web Conference 2022*. 829–837.
- [12] Qian Li, Shu Guo, Yangyifei Luo, Cheng Ji, Lihong Wang, Jiawei Sheng, and Jianxin Li. 2023. Attribute-Consistent Knowledge Graph Representation Learning for Multi-Modal Entity Alignment. In *Proceedings of the ACM Web Conference 2023*. 2499–2508.
- [13] Bing Liu, Harrison Scells, Guido Zuccon, Wen Hua, and Genghong Zhao. 2021. ActiveEA: Active Learning for Neural Entity Alignment. (2021), 3364–3374.
- [14] Yu Liu, Wen Hua, Kexuan Xin, Saied Hosseini, and Xiaofang Zhou. 2023. TEA: Time-aware Entity Alignment in Knowledge Graphs. In *Proceedings of the ACM Web Conference 2023*. 2591–2599.
- [15] Zhiyuan Liu, Yixin Cao, Liangming Pan, Juanzi Li, and Tat-Seng Chua. 2020. Exploring and Evaluating Attributes, Values, and Structures for Entity Alignment. In *Proceedings of the 2020 Conference on Empirical Methods in Natural Language Processing (EMNLP)*. 6355–6364.
- [16] Xinnian Mao, Meirong Ma, Hao Yuan, Jianchao Zhu, Zongyu Wang, Rui Xie, Wei Wu, and Man Lan. 2022. An effective and efficient entity alignment decoding algorithm via third-order tensor isomorphism. In *Proceedings of the 60th Annual Meeting of the Association for Computational Linguistics (Volume 1: Long Papers)*. 5888–5898.
- [17] Xin Mao, Wenting Wang, Yuanbin Wu, and Man Lan. 2021. Are negative samples necessary in entity alignment? an approach with high performance, scalability and robustness. In *Proceedings of the 30th ACM International Conference on Information & Knowledge Management*. 1263–1273.
- [18] Xin Mao, Wenting Wang, Yuanbin Wu, and Man Lan. 2021. Boosting the speed of entity alignment 10x: Dual attention matching network with normalized hard sample mining. In *Proceedings of the Web Conference 2021*. 821–832.
- [19] Xin Mao, Wenting Wang, Huimin Xu, Man Lan, and Yuanbin Wu. 2020. MRAEA: an efficient and robust entity alignment approach for cross-lingual knowledge graph. In *Proceedings of the 13th International Conference on Web Search and Data Mining*. 420–428.
- [20] Xin Mao, Wenting Wang, Huimin Xu, Yuanbin Wu, and Man Lan. 2020. Relational reflection entity alignment. In *Proceedings of the 29th ACM International Conference on Information & Knowledge Management*. 1095–1104.
- [21] Lawrence Page, Sergey Brin, Rajeev Motwani, and Terry Winograd. 1998. *The pagerank citation ranking: Bring order to the web*. Technical Report. Technical report, stanford University.
- [22] Shichao Pei, Lu Yu, Robert Hoehndorf, and Xiangliang Zhang. 2019. Semi-supervised entity alignment via knowledge graph embedding with awareness of degree difference. In *The world wide web conference*. 3130–3136.
- [23] Bryan Perozzi, Rami Al-Rfou, and Steven Skiena. 2014. Deepwalk: Online learning of social representations. In *Proceedings of the 20th ACM SIGKDD international conference on Knowledge discovery and data mining*. 701–710.
- [24] Meng Qu, Jian Tang, and Yoshua Bengio. 2019. Weakly-supervised Knowledge Graph Alignment with Adversarial Learning. *CoRR abs/1907.03179* (2019).
- [25] Yousef Saad. 2011. *Numerical methods for large eigenvalue problems: revised edition*. SIAM.
- [26] Zequn Sun, Muhao Chen, and Wei Hu. 2021. Knowing the No-match: Entity Alignment with Dangling Cases. In *Proceedings of the 59th Annual Meeting of the Association for Computational Linguistics and the 11th International Joint Conference on Natural Language Processing (Volume 1: Long Papers)*. 3582–3593.
- [27] Zequn Sun, Wei Hu, Qingheng Zhang, and Yuzhong Qu. 2018. Bootstrapping entity alignment with knowledge graph embedding. In *IJCAI*, Vol. 18.
- [28] Zequn Sun, Jiacheng Huang, Xiaozhou Xu, Qijin Chen, Weijun Ren, and Wei Hu. 2023. What Makes Entities Similar? A Similarity Flooding Perspective for Multi-sourced Knowledge Graph Embeddings. *arXiv preprint arXiv:2306.02622* (2023).
- [29] Anil Surisetty, Deepak Chaurasiya, Nitish Kumar, Alok Singh, Gaurav Dhama, Aakarsh Malhotra, Ankur Arora, and Vikrant Dey. 2022. Reps: Relation, position and structure aware entity alignment. In *Companion Proceedings of the Web*

- Conference 2022. 1083–1091.
- [30] Wei Tang, Fenglong Su, Haifeng Sun, Qi Qi, Jingyu Wang, Shimin Tao, and Hao Yang. 2023. Weakly Supervised Entity Alignment with Positional Inspiration. In *Proceedings of the Sixteenth ACM International Conference on Web Search and Data Mining*. 814–822.
- [31] Bayu Distiawan Trisedya, Jianzhong Qi, and Rui Zhang. 2019. Entity alignment between knowledge graphs using attribute embeddings. In *Proceedings of the AAAI conference on artificial intelligence*, Vol. 33. 297–304.
- [32] Anton Tsitsulin, Davide Mottin, Panagiotis Karras, and Emmanuel Müller. 2018. Verse: Versatile graph embeddings from similarity measures. In *Proceedings of the 2018 world wide web conference*. 539–548.
- [33] Petar Velickovic, Guillem Cucurull, Arantxa Casanova, Adriana Romero, Pietro Liò, and Yoshua Bengio. 2017. Graph Attention Networks. *CoRR* abs/1710.10903 (2017).
- [34] Sheng Wan, Shirui Pan, Jian Yang, and Chen Gong. 2021. Contrastive and generative graph convolutional networks for graph-based semi-supervised learning. In *Proceedings of the AAAI conference on artificial intelligence*, Vol. 35. 10049–10057.
- [35] Jihu Wang, Yuliang Shi, Han Yu, Xinjun Wang, Zhongmin Yan, and Fanyu Gong. 2023. Mixed-Curvature Manifolds Interaction Learning for Knowledge Graph-aware Recommendation. In *Proceedings of the 46th International ACM SIGIR Conference on Research and Development in Information Retrieval*. 372–382.
- [36] Yuanyi Wang, Haifeng Sun, Jingyu Wang, Qi Qi, Shaoling Sun, and Jianxin Liao. 2024. Gradient Flow of Energy: A General and Efficient Approach for Entity Alignment Decoding. *arXiv preprint arXiv:2401.12798* (2024).
- [37] Yuanyi Wang, Haifeng Sun, Jiabo Wang, Jingyu Wang, Wei Tang, Qi Qi, Shaoling Sun, and Jianxin Liao. 2024. Towards Semantic Consistency: Dirichlet Energy Driven Robust Multi-Modal Entity Alignment. *arXiv preprint arXiv:2401.17859* (2024).
- [38] Zhichun Wang, Qingsong Lv, Xiaohan Lan, and Yu Zhang. 2018. Cross-lingual knowledge graph alignment via graph convolutional networks. In *Proceedings of the 2018 conference on empirical methods in natural language processing*. 349–357.
- [39] Y Wu, X Liu, Y Feng, Z Wang, R Yan, and D Zhao. 2019. Relation-Aware Entity Alignment for Heterogeneous Knowledge Graphs. In *Proceedings of the Twenty-Eighth International Joint Conference on Artificial Intelligence*. International Joint Conferences on Artificial Intelligence.
- [40] Zonghan Wu, Shirui Pan, Fengwen Chen, Guodong Long, Chengqi Zhang, and S Yu Philip. 2020. A comprehensive survey on graph neural networks. *IEEE transactions on neural networks and learning systems* 32, 1 (2020), 4–24.
- [41] Kexuan Xin, Zequn Sun, Wen Hua, Wei Hu, Jianfeng Qu, and Xiaofang Zhou. 2022. Large-scale entity alignment via knowledge graph merging, partitioning and embedding. In *Proceedings of the 31st ACM International Conference on Information & Knowledge Management*. 2240–2249.
- [42] Kai Yang, Shaoqin Liu, Junfeng Zhao, Yasha Wang, and Bing Xie. 2020. COTSAE: co-training of structure and attribute embeddings for entity alignment. In *Proceedings of the AAAI Conference on Artificial Intelligence*, Vol. 34. 3025–3032.
- [43] Renchi Yang, Jieming Shi, Xiaokui Xiao, Yin Yang, and Sourav S Bhowmick. [n. d.]. Homogeneous Network Embedding for Massive Graphs via Reweighted Personalized PageRank. *Proceedings of the VLDB Endowment* 13, 5 ([n. d.]).
- [44] Yuan Yin and Zhewei Wei. 2019. Scalable graph embeddings via sparse transpose proximities. In *Proceedings of the 25th ACM SIGKDD International Conference on Knowledge Discovery & Data Mining*. 1429–1437.
- [45] Donghan Yu and Yiming Yang. 2023. Retrieval-Enhanced Generative Model for Large-Scale Knowledge Graph Completion. In *Proceedings of the 46th International ACM SIGIR Conference on Research and Development in Information Retrieval*. 2334–2338.
- [46] Weixin Zeng, Xiang Zhao, Jiuyang Tang, and Changjun Fan. 2021. Reinforced active entity alignment. In *Proceedings of the 30th ACM International Conference on Information & Knowledge Management*. 2477–2486.
- [47] Ziwei Zhang, Peng Cui, Xiao Wang, Jian Pei, Xuanrong Yao, and Wenwu Zhu. 2018. Arbitrary-order proximity preserved network embedding. In *Proceedings of the 24th ACM SIGKDD international conference on knowledge discovery & data mining*. 2778–2786.
- [48] Xiang Zhao, Weixin Zeng, Jiuyang Tang, Wei Wang, and Fabian M Suchanek. 2020. An experimental study of state-of-the-art entity alignment approaches. *IEEE Transactions on Knowledge and Data Engineering* 34, 6 (2020), 2610–2625.
- [49] Yao Zhu, Hongzhi Liu, Zhonghai Wu, and Yingpeng Du. 2021. Relation-Aware Neighborhood Matching Model for Entity Alignment. In *Thirty-Fifth AAAI Conference on Artificial Intelligence, AAAI 2021, Thirty-Third Conference on Innovative Applications of Artificial Intelligence, IAAI 2021, The Eleventh Symposium on Educational Advances in Artificial Intelligence, EAAI 2021, Virtual Event, February 2-9, 2021*. AAAI Press, 4749–4756.

A THEORETICAL RESULTS

A.1 Proof of Proposition 3.1

PROOF. Consider Equation 1, which represents an entity as a composition of other entities:

$$x_i = \sum_{j=1}^n \lambda_{i,j} x_j \quad (21)$$

Here, x_i represents an entity in the source knowledge graph \mathcal{E}_s , and x_j represents neighboring entities. The coefficients $\lambda_{i,j}$ determine the propagation weights and can be computed as:

$$\lambda_{i,j} = \frac{\mathcal{B}_{(x_i, x_j) \in \mathcal{N}}}{|\mathcal{N}_{x_i}|} \quad (22)$$

In the above equation, \mathcal{B} is an indicator function that returns 1 if there exists a relation between x_i and x_j and 0 otherwise. The similarity between entities $x_i \in \mathcal{E}_s$ and $y_i \in \mathcal{E}_t$ can be calculated using the inner product as follows:

$$\omega_{i,j} = x_i \cdot y_j = \sum_{k=1}^n \sum_{l=1}^m \lambda_{i,k}^s \lambda_{j,l}^t x_k \cdot y_l = \sum_{k=1}^n \sum_{l=1}^m \lambda_{i,k}^s \lambda_{j,l}^t \omega_{k,l} \quad (23)$$

The above equation illustrates how the similarity between two entities is influenced by their associated neighbors.

Now, we can denote the pairwise entity similarities of the two knowledge graphs as $\Omega = (\omega_{i,j})_{i=1, j=1}^{n,m}$. We can also construct matrices $\Lambda^s = (\lambda_{i,j}^s)_{i=1, j=1}^{n,n}$ for the source knowledge graph, and $\Lambda^t = (\lambda_{i,j}^t)_{i=1, j=1}^{m,m}$ for the target knowledge graph, where these matrices serve as propagation operators. In Equation 24, we introduce constraints on the propagation matrix Λ . Specifically, we impose the condition that the sum of every row element equals 1. Each element $\lambda_{i,j}$ within this matrix represents the probability governing the propagation of information from entity x_i to entity x_j .

$$|\Lambda(i, :)| = \sum_{j=1}^n \lambda_{i,j} = \frac{\sum_{j=1}^n |\mathcal{B}(x_i, x_j) \in \mathcal{N}|}{|\mathcal{N}_{x_i}|} = 1 \quad (24)$$

Consequently, we establish the relationship $\Lambda^s \Omega (\Lambda^t)^\top = \Omega$, where Λ assumes the role of a random walk strategy facilitating the propagation of information encoded within the similarity matrix Ω . This propagation operator, denoted as Λ , can be effectively employed within an iterative strategy, making use of its properties pertaining to fixpoints as required. \square

A.2 Proof of Proposition 3.2

PROOF. We aim to show that the complementary events, namely $\text{rank}(\Lambda \Lambda^\top) < n$, have zero probability. Let's take $Y = \Lambda \Lambda^\top$ as an example. It follows that $\text{rank}(Y) < n$ if and only if $\text{rank}(Y^\top Y) < n$. This occurs if and only if $\det(Y^\top Y) = 0$. Therefore, we need to demonstrate that the probability of the event $\det(Y^\top Y) = 0$ is zero. Let us denote

$$g(Y) = \det(Y^\top Y) \quad (25)$$

where g is a polynomial. We are interested in the probability of its zero-level set. However, the zero-level set of a non-zero polynomial has zero Lebesgue measure. In our case, g is not the constant zero

Table 4: Datasets statistics.

	Cross-Lingual Datasets						Mono-Lingual Datasets					
	15K-EN	15K-FR	15K-EN	15K-DE	100K-EN	100K-FR	15K-DBP	15K-Wiki	15K-DBP	15K-Yago	100K-DBP	100K-Wiki
Relation	193	166	169	96	379	287	167	121	72	21	318	239
Triple	96318	80112	84867	92632	649902	561391	73983	83365	68063	60970	616457	588203
Anchors	15000	15000	15000	15000	100000	100000	15000	15000	15000	15000	100000	100000
Train	150	150	150	150	1000	1000	150	150	150	150	1000	1000
Test	14850	14850	14850	14850	99000	99000	14850	14850	14850	14850	99000	99000

Table 5: Hyperparameter settings of model.

Models	d	lr	b	η	γ	dr	eps
PSR	300,300	0.005	512	-	1.5,2.0	0.3	40
SEA	100	0.01	5000	10	1.5,2.0	-	2000
MRAEA	50,50	0.001	10000	5	1.0	0.3	5000
KECG	128	0.005	-	1	2.0	-	1000
BootEA	75	0.01	20000	10	-	-	500
RREA	100,100	0.005	15000,100000	5	3.0	0.3	1200
Dual-AMN	128,128	0.005	1024	-	1.0	0.3	100
GCN-Align	300	0.02	-	5	3.0	0	2000
PEEA	128,128,128	0.005	1024	-	15.0	0.3	60
LightEA	1024,1024	-	-	-	-	-	-
Ours	128,128,128	0.005	1024	-	15.0	0.3	60

function since $g(Q) = 1$. Consequently, we have

$$Pr(g(Y) = 0) = \int_{g^{-1}(0)} f(x) dx = 0 \quad (26)$$

where the integral is zero since we integrate over a set with zero measure. Pr represents the probability of an event occurring, and $f(x)$ is the probability density function of x . The meaning of the above equation is that the probability of the event $\det(Y > Y) = 0$ is zero. Thus we prove that

$$\text{rank}(Y) = n \quad (27)$$

Theorem 3.4 in [28] reveals that embedding-based EA models are aimed at identifying fixed-point sets of pairwise entity similarities. These models define an alignment mapping function to align knowledge graph matrices, yielding alignment outcomes. In our context, where we consider these matrices, particularly the similarity matrix, as edge weights between nodes in graphs, these EA models essentially perform mathematical graph matching. The edge weight matrix Ω characterizes the subgraph between entities across graphs in the unified space, which can be viewed as a comprehensive isomorphic graph. As confirmed in the proof of Proposition 3.1, we have $\Lambda^S \Omega (\Lambda^L)^T = \Omega$, and the structure reconstruction process is denoted as $Y = \Lambda \Lambda^T$. According to Eq.27, this reconstruction process guarantees that each node has corresponding matches in another graph. Consequently, it validates the phenomenon that matched nodes in the graph exhibit isomorphic subgraphs suitable for all nodes in the graphs. \square

A.3 Proof of Proposition 3.3

We aim to prove the proposition by demonstrating that we satisfy the assumptions of *Theorem 5.1* [25]. Although the theorem establishes convergence to the Schur vectors $[q_1, \dots, q_k]$ associated with $\lambda_1, \dots, \lambda_k$, it's important to note that for symmetric matrices, these Schur vectors coincide with the k orthogonal eigenvectors.

Let $\hat{\Omega} = [\hat{\Omega}_1, \dots, \hat{\Omega}_k]$. Our objective is to show that

$$\text{rank}(P_i [\hat{\Omega}_1, \dots, \hat{\Omega}_k]) = i \quad (28)$$

where $1 \leq i \leq k$, and P_i represents the spectral projector associated with eigenvalues $\lambda_1, \dots, \lambda_i$. Given the distinctness and simplicity of the eigenvalues (by assumption) and the symmetry of the operator (implying the equivalence of left and right eigenvectors), we can express the spectral projector as:

$$P_i = \sum_{j=1}^i q_j q_j^T \quad (29)$$

Here, we assume without loss of generality that q_j has a unitary norm. Equivalently, we can write $P_i = Q_i Q_i^T$, where $Q_i = [q_1, \dots, q_i]$. Consequently, we need to demonstrate that

$$\text{rank}(Q_i Q_i^T [\hat{\Omega}_1, \dots, \hat{\Omega}_i]) = i \quad (30)$$

where $1 \leq i \leq k$. This occurs with probability 1 according to Proposition 3.2, as shown earlier.

B SINKHORN ITERATION

$$\text{Sink}^{(0)}(\Omega) = \exp(\Omega)$$

$$\text{Sink}^{(q)}(\Omega) = \mathcal{N}_c(\mathcal{N}_r(\text{Sink}^{(q-1)}(\Omega))) \quad (31)$$

$$\text{Sinkhorn}(\Omega) = \lim_{q \rightarrow \infty} \text{Sink}^{(q)}(\Omega)$$

here $\mathcal{N}_r(\Omega) = \Omega \oslash (\Omega \mathbf{1}_N \mathbf{1}_N^T)$ and $\mathcal{N}_c(\Omega) = \Omega \oslash (\mathbf{1}_N \mathbf{1}_N^T \Omega)$ are the row and column-wise normalization operators of a matrix, \oslash represents the element-wise division, and $\mathbf{1}_N$ is a column vector of ones.

C TIME COMPLEXITY

To streamline our analysis, we assume both graphs have 'n' nodes. The propagation process involves two main steps: propagation computation and matrix factorization. The computation of propagation is a pivotal step. Its time complexity is bounded by $\mathcal{O}(m \cdot n \cdot L_1)$, where m represents the number of edges, and L_1 signifies the count of propagation iterations. In the matrix factorization step, extensive calculations are performed on a dense matrix of size $\mathcal{O}(n^2)$. Consequently, the time complexity is $\mathcal{O}(m \cdot n \cdot L_1)$, mainly due to the

computational cost of the former operation. To mitigate this, we introduce an efficient generalized push algorithm, which reduces the complexity to $O\left(\frac{S}{\delta}\right)$, with δ controlling the trade-off between computational expense and proximity matrix sparsity.

The refinement process consists of L_2 ' iterations. In each iteration, our method computes the left and right multiplication of a dense $n \times n$ matching matrix with two adjacency matrices from graphs, each with an average degree denoted as \bar{d}_1, \bar{d}_2 , respectively. Consequently, the time complexity for this update step is $O(n^2(\bar{d}_1 + \bar{d}_2))$. Normalizing the matrix in each iteration and incorporating token match scores requires $O(n^2)$ time. Therefore, the overall time complexity stands at $O(L_2 n^2(\bar{d}_1 + \bar{d}_2))$.

D DATASETS

In our experimental evaluation, we employed six datasets curated within the OpenEA framework [26]. These datasets encompass two cross-lingual settings, namely English-to-French and English-to-German, extracted from the multi-lingual DBpedia. Additionally, we considered two mono-lingual settings derived from well-established knowledge bases, specifically DBpedia-to-Wikidata and DBpedia-to-YAGO. A comprehensive summary of the dataset statistics is provided in Table 4.

E HYPER-PARAMETERS

Our experimental configuration is based on the default optimal settings of various hyperparameters. Specifically, we focus on the following hyperparameters: the number of epochs (eps), learning rates (lr), batch sizes (b), negative sampling rates (η), dropout rates (dr), and the number of GNN layers (L). Our primary focus during experimentation involves a grid search over embedding dimensions (d) and margins (γ). Additionally, we maintain consistency with the original papers when it comes to the number of multi-head attention mechanisms used in models like MRAEA, RREA, and Dual-AMN, which are fixed at two. To conduct our experiments in a rigorous manner, we vary the embedding dimension (d) within the range of (50, 100, 128, 300) and the margin (γ) within the range of (0, 0.5, 1.0, 1.5, 2.0, 2.5, 3.0, 10.0, 15.0, 20.0). It is essential to note that, for the sake of fair comparison, we exclude attributes when employing the GCN-Align method. A comprehensive summary of all hyperparameters employed in our experiments is presented in Table 5.

Received 20 February 2007; revised 12 March 2009; accepted 5 June 2009